Synthesis and In Vitro and In Vivo Evaluation of Hypoxia-Enhanced ^{111}In-Bombesin Conjugates for Prostate Cancer Imaging

Zhengyuan Zhou[1], Nilesh K. Wagh[1], Sunny M. Ogbomo[1], Wen Shi[1], Yinnong Jia[1], Susan K. Brusnahan[1], and Jered C. Garrison[1–4]

[1]*Department of Pharmaceutical Sciences, College of Pharmacy, University of Nebraska Medical Center, Nebraska Medical Center, Omaha, Nebraska;* [2]*Center for Drug Delivery and Nanomedicine, University of Nebraska Medical Center, Nebraska Medical Center, Omaha, Nebraska;* [3]*Department of Biochemistry and Molecular Biology, College of Medicine, University of Nebraska Medical Center, Nebraska Medical Center, Omaha, Nebraska; and* [4]*Eppley Cancer Center, University of Nebraska Medical Center, Nebraska Medical Center, Omaha, Nebraska*

Receptor-targeted agents, such as gastrin-releasing peptide receptor (BB2r)–targeted peptides, have been investigated extensively in preclinical and clinical studies. In an attempt to increase the effectiveness of diagnostic or radiotherapeutic agents, we have begun to explore the incorporation of the hypoxia-selective prodrug 2-nitroimidazole into receptor-targeted peptides. Hypoxia is a well-known characteristic of many solid tumors, including breast, prostate, and pancreatic cancers. The aim of this approach is to use the hypoxia-trapping capability of 2-nitroimidazoles to increase the retention of the agent in hypoxic, BB2r-positive tumors. We have demonstrated that incorporation of one or more 2-nitroimidazoles into the BB2r-targeted peptide significantly increases the in vitro retention of the agent in hypoxic prostate cancer cells. The study described herein represents our first investigation of the in vivo properties of these hypoxia-enhanced BB2r-targeted agents in a PC-3 xenograft mouse model. **Methods:** Four ^{111}In-labeled BB2r-targeted conjugates—**^{111}In-1, ^{111}In-2, ^{111}In-3,** and **^{111}In-4,** composed of 2-nitroimidazole moieties of 0, 1, 2, and 3, respectively—were synthesized, labeled, and purified. The BB2r binding affinities, externalization, and protein-association properties of these radioconjugates were assessed using the BB2r-positive PC-3 human prostate cancer cell line under hypoxic and normoxic environments. The in vivo biodistribution and micro-SPECT/CT imaging of the **^{111}In-1, ^{111}In-2,** and **^{111}In-4** radioconjugates were investigated in PC-3 tumor–bearing severely combined immunodeficient mice. **Results:** All conjugates and ^{nat}In-conjugates demonstrated nanomolar binding affinities. **^{111}In-1, ^{111}In-2, ^{111}In-3,** and **^{111}In-4** demonstrated 41.4%, 60.7%, 69.1%, and 69.4% retention, correspondingly, of internalized radioactivity under hypoxic conditions relative to 34.8%, 35.3%, 33.2%, and 29.7% retention, respectively, under normoxic conditions. Protein-association studies showed significantly higher levels of association under hypoxic conditions for 2-nitroimidazole–containing BB2r-targeted radioconjugates than for controls. On the basis of the initial 1-h uptake in the PC-3 tumors, **^{111}In-1, ^{111}In-2,** and **^{111}In-4** demonstrated tumor retentions of 1.5%, 6.7%, and 21.0%, respectively, by 72 h after injection. Micro-SPECT/CT imaging studies of **^{111}In-1, ^{111}In-2,** and **^{111}In-4** radioconjugates resulted in clear delineation of the tumors. **Conclusion:** On the basis of the in vitro and in vivo studies, the BB2r-targeted agents that incorporated 2-nitroimidazole moieties demonstrated improved retention. These results indicate that further exploration into the potential of hypoxia-selective trapping agents for BB2r-targeted agents, as well as other targeted compounds, is warranted.

Key Words: tumor hypoxia; bombesin; BB2 receptor; prostate cancer; 2-nitroimidazole

J Nucl Med 2013; 54:1605–1612
DOI: 10.2967/jnumed.112.117986

According to the American Cancer Society estimates, prostate cancer is the second leading cause of death and accounts for 29% of all new cancer cases for men in the United States (*1*). The gastrin-releasing peptide receptor (BB2r) has been thoroughly investigated as a diagnostic and therapeutic target for prostate and other cancers because of the high expression of the receptor on neoplastic relative to normal tissues (*2,3*). To date, a variety of BB2r-targeted agents have been developed using the BBN(7-14) NH_2 sequence (Gln-Trp-Ala-Val-Gly-His-Leu-Met-NH_2) (*4–7*). The developed BB2r-targeted agents, as with most low-molecular-weight, receptor-targeted drugs, demonstrate rapid targeting of receptor-positive tumors and swift clearance from nontargeted tissues. However, the disadvantage of many of these agents is low retention at the tumor site because of intrinsically high diffusion and efflux rates. The lower tumor retention can substantially reduce the diagnostic and therapeutic efficacy of the agent and its potential for clinical translation.

Tissue hypoxia is the result of an inadequate supply of oxygen. In most solid cancers, hypoxic regions commonly exist because of a chaotic vascular architecture, which impedes delivery of oxygen and other nutrients. A recent clinical investigation found that 63% (median, $n = 247$) of prostate tumors gave pO_2 measurements of less than 1.3 kPa (10 mm Hg; tissues less than this are generally defined as hypoxic) (*8*). The extent of hypoxia in tumors appears to be strongly associated with the aggressiveness of the tumor phenotype, therapeutic resistance, and patient prognosis (*9*). Because hypoxia is not present in most normal human tissues, a variety of bioreductive, hypoxia-selective prodrugs has been

Received Nov. 30, 2012; revision accepted Mar. 27, 2013.
For correspondence or reprints contact: Jered C. Garrison, University of Nebraska Medical Center, DRC1 Rm. 4008, 985830 Nebraska Medical Center, Omaha, NE 68198-5830.
E-mail: jcgarrison@unmc.edu
Published online Jul. 29, 2013.

developed for the purpose of diagnostic and therapeutic applications for cancer. Nitroimidazoles have been used extensively in basic and clinical investigation as diagnostic imaging agents (*10,11*). In hypoxic environments, nitroimidazoles undergo a series of enzymatic reductions—mediated by nitroreductase enzymes—leading to the formation of strong electrophiles, which can irreversibly bind to intracellular nucleophiles, thereby trapping the agent in the hypoxic tissue (*12*). Recently, radiohalogenated nitroimidazoles, such as ^{18}F-fluoromisonidazole, ^{18}F-1-α-D-(2-deoxy-2-fluoroarabinofuranosyl)-2-nitroimidazole, and ^{123}I-iodoazomycin arabinoside, have been used clinically to detect hypoxia in tumors (*13–15*).

One focus of our laboratory is the development of tumor-selective chemical moieties to increase the retention of receptor-targeted agents. We have begun investigating the inclusion of 2-nitroimidazoles into the structure of BB2r-targeted peptides. We have previously demonstrated that these hypoxia-enhanced BB2r-targeted peptides significantly increase retention in hypoxic PC-3 human prostate cancer cells (*16*). From these studies, it was determined that the proximity of the 2-nitroimidazole relative to the pharmacophore had a substantial impact on BB2r binding affinity. Herein, we present the synthesis and in vitro properties of hypoxia-enhanced BB2r-targeted radioconjugates with extended linking groups to improve BB2r binding affinity. Additionally, using biodistribution and micro-SPECT/CT imaging studies, we report the first, to our knowledge, in vivo investigation of these agents in a PC-3 xenograft mouse model.

MATERIALS AND METHODS

Full details regarding the chemicals, equipment, and methodology used in this manuscript are presented in the supplemental materials (available at http://jnm.snmjournals.org).

Cell Lines and Xenograft Models

Prostate cancer (PC-3) cell lines were obtained from American Type Culture Collection and cultured under vendor-recommended conditions. All animal experiments were conducted in accordance with the Principles of Animal Care outlined by National Institutes of Health and approved by the Institutional Animal Care and Use Committee of the University of Nebraska Medical Center. Four-week-old Institute of Cancer Research severely combined immunodeficient (SCID) mice were obtained from Charles River Laboratories. Food and water were given ad libitum. Each animal was kept in individual cages equipped with a HEPA air filter cover in a light- and temperature-controlled environment. Bilateral PC-3 tumors were induced by subcutaneous injection of 5.0×10^6 cells in Matrigel (BD Biosciences). The tumors were allowed to grow to 0.1–1 g (4–6 wk after inoculation) before the mice were used in pharmacokinetic studies.

Synthesis and Radiolabeling of 2-Nitroimidazole Acetic Acid (2-NIAA) Bombesin Conjugates

Peptides 1, 2*, 3*, and 4* were synthesized using an automated solid-phase peptide synthesizer (CEM) with traditional Fmoc chemistry using a Rink Amide resin (Nova Biochem). Electrospray mass spectrometry was used to determine the molecular mass of the prepared peptides. All conjugates were peak-purified to 95% or greater purity and quantified by reversed-phase high-performance liquid chromatography (RP-HPLC) before in vitro and in vivo investigations. The 2-NIAA was synthesized as previously described (*16*). The 2-NIAA was manually coupled to the ε-amino group of the lysine residue for peptides **2*, 3***, and **4*** using standard amidation chemistry, peak-purified by RP-HPLC, and characterized by mass spectrometry. For the convenient characterization of the ^{111}In-bombesin conjugates, naturally abundant ^{nat}In was used to substitute for ^{111}In in the electrospray mass spectrometry and in vitro binding studies. Isolated yields were 57.6%, 28.4%, 56.8%, and 40.4% for **^{nat}In-1, ^{nat}In-2, ^{nat}In-3,** and **^{nat}In-4,** respectively. All ^{nat}In-conjugates were of 95% or greater purity before mass spectrometric characterization. Radiolabeling was performed on all conjugates by mixing 100-μg samples with 37 MBq of $^{111}InCl_3$ in ammonium acetate buffer (1 M, 200 μL, pH 5.5). The solution was heated for 60 min at 90°C. The resulting specific radioactivities were 0.64, 0.71, 0.78, and 0.86 MBq/nmol for **^{111}In-1, ^{111}In-2, ^{111}In-3,** and **^{111}In-4,** respectively. To separate radiolabeled peptides from unlabeled peptides on HPLC, 4–5 mg of $CoCl_2$ were then added and incubated for 5 min at 90°C to increase the hydrophobicity of unlabeled conjugates. The solutions were allowed to cool to room temperature, peak-purified using RP-HPLC (≥95%), and concentrated using a C_{18} extraction disk (3M Empore). The specific activities for all peak-purified ^{111}In-conjugates are essentially the theoretic maximum of 1,725 MBq/nmol. Radiolabeling yields for **^{111}In-1, ^{111}In-2, ^{111}In-3,** and **^{111}In-4** were 86.3%, 45.2%, 71.1%, and 58.8%, respectively.

In Vitro Studies

The inhibitory concentration (IC_{50}) for all conjugates and ^{nat}In-conjugates was determined using the PC-3 human prostate cancer cell line. ^{nat}In-conjugates were used as substitutes for the corresponding ^{111}In-radioconjugates. The cell-associated activity was measured using a γ-counter (LTI). Efflux studies were performed using PC-3 cells, which were incubated in 6-well plates (0.5×10^6/well) under hypoxic conditions (94.9% N_2, 0.1% O_2, 5% CO_2) overnight. On the day of the experiment, the medium was replaced with fresh normoxic or hypoxic medium and incubated for 2 h under normoxic (95% air, 5% CO_2) and hypoxic conditions, respectively. The cells were preincubated for 2 h at 37°C in the presence of 100,000 cpm of each ^{111}In-radioconjugate. At time points 0, 2, 4, and 8 h, the radioactivity of the effluxed, surface-bound, and internalized fractions for each radioconjugate was collected and determined using a γ-counter. For the cellular fractionation studies, normoxic and hypoxic PC-3 cells (2.5×10^5/well) were prepared as outlined in the efflux studies above. At time points 2, 4, and 8 h, the cells were lysed and transferred to an Amicon Ultracel 30-kDa filter with extra phosphate-buffered saline (1 mL). The samples were centrifuged at 4,000*g* for 10 min and washed with phosphate-buffered saline (1 mL × 2). The radioactivity associated with the molecular-weight fractions was collected and determined using a γ-counter.

Biodistribution and Small-Animal SPECT/CT Imaging Studies

Biodistribution studies were performed using PC-3 tumor–bearing SCID mice. Each mouse (average weight, 20 g) received an intravenous bolus injection via the tail of 277.5 kBq (7.5 μCi) of the radio–RP-HPLC peak-purified ^{111}In-radioconjugate (**^{111}In-1, ^{111}In-2,** or **^{111}In-4**) in 100 μL of saline. The mice were sacrificed, and their tissues were excised at 1, 4, 24, 48, and 72 h after injection. The excised tissues were weighed, the radioactivity measured, and the percentage injected dose (ID) or percentage ID per gram (%ID/g) calculated for each tissue. Blocking studies were also investigated on ^{111}In-4 by coinjection with 300 μg of unlabeled conjugate 4 ($n = 3$). The mice for SPECT/CT imaging studies were administered 4–11 MBq (0.108–0.300 mCi) of the desired BB2r-targeted peptide in 100–200 μL of saline via tail vein injection. At 1, 24, 48, and 72 h after injection, mice were anesthetized with 1%–1.5% isoflurane delivered in a 2:1 mixture of nitrous oxide: oxygen. Images were acquired using a FLEX Triumph CT/SPECT system (SPECT/CT) and software (Gamma Medica, Inc.) fitted with a 5-pinhole (1.0 mm/pinhole) collimator. SPECT projections (30- to

90-min acquisition time per mouse based on the amount of activity) were acquired and reconstructed using SpectReconstructionApp (Gamma Medica, Inc.), followed by CT scans that were acquired and reconstructed using Triumph X-O 4.1 (Gamma Medica, Inc.).

Statistical Analysis

IC_{50} values were determined by nonlinear regression using the 1-binding-site model of GraphPad PRISM 5 (GraphPad Software, Inc). Comparisons of the 2 groups for efflux studies, cellular protein analysis studies, and biodistribution studies were analyzed by the 2-tailed Student *t* test, and *P* values of less than 0.05 were considered statistically significant.

RESULTS

Conjugate Synthesis and Radiolabeling

Four radioconjugates were synthesized using the DOTA-**X**-8-AOC-BBN(7-14)NH_2 paradigm (Fig. 1). The yields of conjugates **1**, **2***, **3***, and **4*** ranged from 16.67% to 20.44% as determined by RP-HPLC. The 2-NIAA coupling of conjugates **2*** and **4*** was performed by *O*-benzotriazole-*N,N,N′,N′*-tetramethyl-uronium-hexafluoro-phosphate (HBTU) conjugation, whereas conjugate **3*** was coupled using *N,N′*-dicyclohexylcarbodiimide. All attempts to conjugate **3*** with 2-NIAA using HBTU resulted in poor yields (<1%). The products were purified by RP-HPLC and isolated with yields of 17.4%, 26.7%, and 19.0% for conjugates **2**, **3,** and **4,** respectively. RP-HPLC retention time and mass spectrometric identification of the conjugates are listed in Table 1.

In Vitro Competitive Cell-Binding Studies

The BB2r binding affinity of the conjugates and ^{nat}In-conjugates were investigated by competitive binding studies using the BB2r-positive, PC-3 cell line. All conjugates and ^{nat}In-conjugates demonstrated nanomolar binding affinities. The ^{nat}In-labeled conjugates had IC_{50} values of 7.1 ± 1.1, 7.3 ± 1.1, 5.8 ± 1.1, and 6.9 ± 1.2 nM for ^{nat}In-1, ^{nat}In-2, ^{nat}In-3, and ^{nat}In-4, respectively. Slightly lower binding affinities were observed for unlabeled conjugates than for ^{nat}In-labeled.

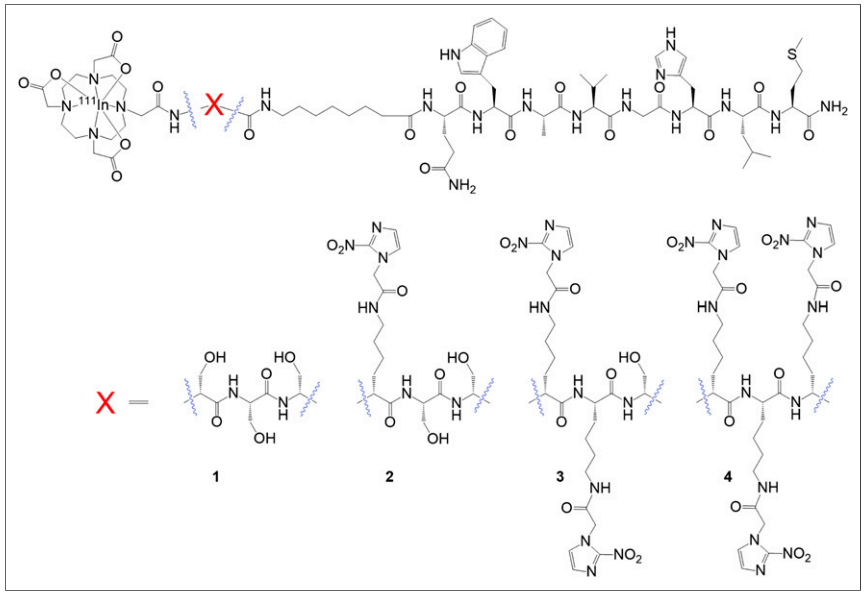

FIGURE 1. Hypoxia-enhanced ^{111}In-BB2r–targeted conjugates.

In Vitro Internalization and Efflux Studies

We have previously reported that the surface expression of the BB2r remains essentially unchanged under the hypoxic conditions used in our studies (*16*). In these studies, **^{111}In-1,** which does not have a 2-nitroimidazole incorporated, is the control to compare the relative effectiveness of the hypoxia-trapping conjugates (**^{111}In-2–4**). The PC-3 cells were first incubated in the presence of the radioconjugates for 2 h before the start of the efflux studies. During this incubation period, all of the radioconjugates investigated under both normoxic and hypoxic conditions demonstrated similar levels of internalization, ranging from 18% to 22% of the total radioactivity added.

The efflux of the radioconjugates over time given as a percentage of the initial internalized activity is depicted in Figure 2. Within the first 2 h of the experiment, the ^{111}In radioconjugates **1–4** under hypoxic conditions demonstrated a lower efflux rate relative to normoxic conditions. At 8 h after incubation, 41.4%, 60.7%, 69.1%, and 69.4% of the initially internalized radioactivity for **^{111}In-1, ^{111}In-2, ^{111}In-3,** and **^{111}In-4,** respectively, was retained under hypoxic conditions, compared with only 34.8%, 35.3%, 33.2%, and 29.7% retained under normoxic conditions. **^{111}In-1** also exhibited a significant decrease in clearance rate after 2 h under hypoxic conditions. However, the increased retention showed by **^{111}In-1** is limited relative to **^{111}In-2–4,** which have 2-nitroimidazoles incorporated into the structure of the radioconjugate. The radioconjugates **^{111}In-2–4** demonstrated significantly higher retention under hypoxic conditions than normoxic conditions ($P < 0.0001$).

The internalized activity of the radioconjugate was compared as an additional means of evaluating the retention effect under normoxic and hypoxic conditions. Hypoxia enhancement factor (HEF) is defined as the ratio of the amount of activity remaining in the hypoxic cells versus the normoxic PC-3 cells of radioconjugates internalized. The HEF for each radioconjugate at each time point is depicted in Figure 3. At the initial time point, all of the radioconjugates demonstrated a similar accumulation under both normoxic and hypoxic conditions where the HEF is approximately equal to 1. At the 2-h time point, all of the radioconjugates incorporated with 2-nitroimidazole started to display significantly higher retention in hypoxic than normoxic cells (i.e., HEF > 1). By the 8-h time point, the **^{111}In-1, ^{111}In-2, ^{111}In-3,** and **^{111}In-4** demonstrated an average HEF of 1.17 ± 0.12, 1.95 ± 0.28, 2.72 ± 0.35, and 3.29 ± 0.25, respectively. The radioconjugates **^{111}In-2–4** exhibited significantly higher average HEF ratios than the control. The strong positive linear relationship between the HEF and the number of 2-nitroimidazoles incorporated was confirmed by linear regression analysis ($R > 0.96$).

Cellular Protein Analysis

It is well established that 2-nitroimidazoles are reductively activated in a hypoxic environment. This activation leads to the irreversible conjugation of the reduced 2-nitroimidazole moiety with intracellular nucleophiles (e.g., thiols), including those contained in proteins, to form adducts

TABLE 1
Mass Spectrometric and RP-HPLC Characterization of Conjugates

Conjugate	Analog	Molecular formula	Mass calculated	Mass observed	RP-HPLC retention time†/min	IC_{50}‡/nM
1	DOTA-(D)S-(D)S-(D)S-8 AOC–BBN(7-14) NH_2	$C_{76}H_{121}N_{21}O_{23}S$	1,728.9	1,729.6	12.08	11.3 ± 1.4
2*	DOTA-(D)K-(D)S-(D)S-8 AOC–BBN(7-14) NH_2	$C_{79}H_{128}N_{22}O_{22}S$	1,770.1	1,770.8	7.73	—
3*	DOTA-(D)K-(D)K-(D)S-8 AOC–BBN(7-14) NH_2	$C_{82}H_{135}N_{23}O_{21}S$	1,811.1	1,812.1	12.37	—
4*	DOTA-(D)K-(D)K-(D)K-8 AOC–BBN(7-14) NH_2	$C_{85}H_{142}N_{24}O_{20}S$	1,852.2	1,852.5	9.32	—
2	DOTA [(D)K (2-NIAA)–(D)S-(D)S-8 AOC]–BBN(7-14) NH_2	$C_{84}H_{131}N_{25}O_{25}S$	1,923.1	1,923.9	14.5	12.6 ± 1.4
3	DOTA [(D)K (2-NIAA)–(D)K (2-NIAA)-(D)S-8 AOC-BBN(7-14) NH_2	$C_{92}H_{141}N_{29}O_{27}S$	2,117.3	2,118.1	8.48	17.1 ± 1.2
4	DOTA [(D)K (2-NIAA)–(D)K (2-NIAA)-(D)K (2-NIAA)-8 AOC]–BBN(7-14) NH_2	$C_{100}H_{151}N_{33}O_{29}S$	2,311.5	2,312.0	9.87	20.1 ± 1.3
In-1	In-DOTA-(D)S-(D)S-(D)S-8 AOC–BBN(7-14) NH_2	$C_{76}H_{118}{}^{114}InN_{21}O_{23}S$	1,839.7	1,840.2§	5.60	7.1 ± 1.1
In-2	In-DOTA [(D)K (2-NIAA)–(D)S-(D)S-8 AOC]–BBN(7-14) NH_2	$C_{84}H_{128}{}^{114}InN_{25}O_{25}S$	2,034.9	2,035.0§	7.87	7.3 ± 1.1
In-3	In-DOTA [(D)K (2-NIAA)–(D)K (2-NIAA)-(D)S-8 AOC-BBN(7-14) NH_2	$C_{92}H_{138}{}^{114}InN_{29}O_{27}S$	2,229.1	2,229.5§	9.2	5.8 ± 1.1
In-4	In-DOTA [(D)K (2-NIAA)–(D)K (2-NIAA)–(D)K (2-NIAA)-8 AOC]–BBN(7-14) NH_2	$C_{100}H_{148}{}^{114}InN_{33}O_{29}S$	2,423.3	2,423.1§	10.55	6.9 ± 1.2

†RP-HPLC methods described in supplemental materials.
‡Values represent mean ± SEM (n = 6).
§For convenient mass spectra analysis ^{111}In was replaced by ^{nat}In.

(*11,17,18*). To better elucidate the mechanism of the observed increase in retention of the 2-nitroimidazole–containing BB2r-targeted agents under hypoxic conditions, the protein-association properties of the conjugates were evaluated under hypoxic and normoxic environments. At the 2-, 4-, and 8-h postincubation time points, the PC-3 cells were lysed and centrifuged. The supernatant was then filtered using a 30-kDa centrifugal filter. The ratio of protein-associated radioactivity as a percentage of total intracellular radioactivity under hypoxic conditions over the percentage of protein-associated radioactivity under a normoxic environment is depicted in Figure 4. The control radioconjugate **^{111}In-1** demonstrated similar ratios, from 1.08 to 1.38, during the timespan of the experiment. The 2-nitroimidazole–containing BB2r-targeted conjugates demonstrated at least 1-fold-higher protein association under hypoxic conditions than that observed under normoxic conditions. For **^{111}In-4,** at the 4- and 8-h time points, up to 3-fold-higher hypoxic/normoxic protein-association ratios were observed relative to the control. These results strongly suggest that 2-nitroimidazoles are partially responsible for this enhancement.

Biodistribution Studies

The in vivo biodistributions of the **^{111}In-1, ^{111}In-2,** and **^{111}In-4** radioconjugates were investigated in PC-3 tumor–bearing SCID mice. Because of the similar efflux and protein-association properties of **^{111}In-3** and **^{111}In-4, ^{111}In-3** was not investigated in vivo. The results obtained from pharmacokinetic studies of **^{111}In-1, ^{111}In-2,** and **^{111}In-4** at 1, 4, 24, 48, and 72 h after injection are summarized in Table 2. All of the investigated ^{111}In-radioconjugates demonstrated rapid blood clearance at 1 h after injection. Clearance of the radioconjugates proceeded largely through the renal or urinary system. At 1 h after injection, the highest accumulation was found in the pancreas for radioconjugates **^{111}In-1, ^{111}In-2,** and **^{111}In-4** (70.96 ± 15.88, 33.70 ± 27.11, and 33.04 ± 19.50 %ID/g, respectively). These results are due to the high expression of BB2r in rodent pancreas and are consistent with previous reports (*5,19*). The tumor retention of radioconjugate **^{111}In-4** (2.80 ± 1.18 %ID/g) at 1 h after injection is substantially lower than **^{111}In-1** (5.82 ± 2.63 %ID/g) and **^{111}In-2** (6.06 ± 3.35 %ID/g). However, by the 72-h postinjection time point, 1.5%, 6.7%, and 21.0% (corresponding to radioconjugates **^{111}In-1, ^{111}In-2,** and **^{111}In-4,** respectively) of the initial 1-h uptake was retained in the tumor tissue (Fig. 5). The tumor retention observed for both **^{111}In-2** (0.41 ± 0.07 %ID/g, $P < 0.01$) and **^{111}In-4** (0.60 ± 0.40 %ID/g, $P < 0.05$) was found to be significantly higher than for the control **^{111}In-1** (0.09 ± 0.10 %ID/g). With the exception of the kidneys, the addition of the 2-nitroimidazoles did not increase the nontarget retention of the BB2r-targeted agents. The initial kidney uptake for all of the radioconjugates investigated was approximately 15 %ID/g at the 1-h time point. By 72 h after injection, the conjugates **^{111}In-2** (2.66 ± 0.73 %ID/g) and **^{111}In-4** (8.83 ± 5.69 %ID/g), as compared with **^{111}In-1** (0.76 ± 0.67 %ID/g), demonstrated significant retention ($P < 0.05$) in the kidneys. In this study, the kidney retention correlated with an increase in the 2-nitroimidazole moieties of the BB2r-targeted agent. The coinjection of an excess of unlabeled conjugate **4** along with ^{111}In-4 resulted in significantly reduced radioactivity in the pancreas (1.16 ± 0.66 %ID/g), kidney

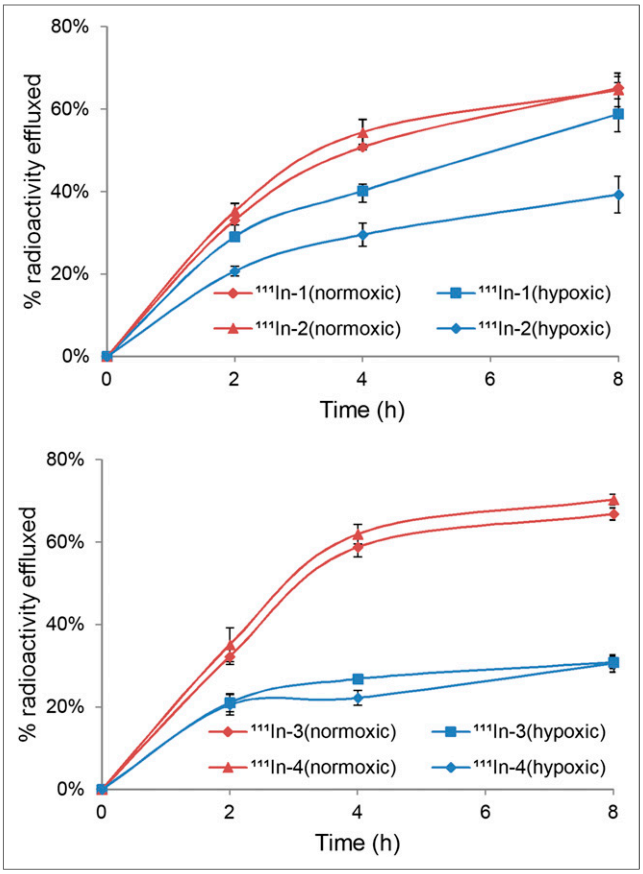

FIGURE 2. Efflux assays depicted as percentage of initial internalized activity for ^{111}In-radioconjugates in PC-3 cells. Values are mean ± SD (n = 5).

(12.37 ± 7.92 %ID/g), and tumor (0.44 ± 0.34 %ID/g) at 4 h after injection ($P < 0.05$, 1-tailed).

Small-Animal SPECT/CT Imaging Studies

Small-animal SPECT/CT imaging studies were performed in PC-3 tumor–bearing SCID mice using the **^{111}In-1, ^{111}In-2,** and **^{111}In-4** radioconjugates. The whole-body images and the respective axial slices of the PC-3 tumors at 1, 24, 48, and 72 h after injection are depicted in Figure 6. At 1 h after injection, significant abdominal uptake was observed in all cases due to the accumulation of radioactivity in the gastrointestinal tract and pancreas, as previously demonstrated in the biodistribution studies. Axial slices of the PC-3 tumor for all the radioconjugates investigated exhibited substantial accumulation of radioactivity in the tumor tissue after the rapid clearance of the radioconjugates through the renal or urinary system. For **^{111}In-4** radioconjugates, conspicuous kidney retention was observed, echoing the biodistribution studies.

DISCUSSION

To determine whether the incorporation of 2-nitroimidazoles would increase the retention of the radioconjugate in hypoxic PC-3 cells, we have previously synthesized 4 BB2r-targeted agents, which included 2-nitroimidazole moieties (*16*). In vitro studies showed improved longitudinal retention of the 2-nitroimidazole–containing BB2r-targeted agents in hypoxic relative to normoxic PC-3 cells. However, it was determined that the steric interference of the 2-nitroimidazole with the BB2r-targeting vector resulted in

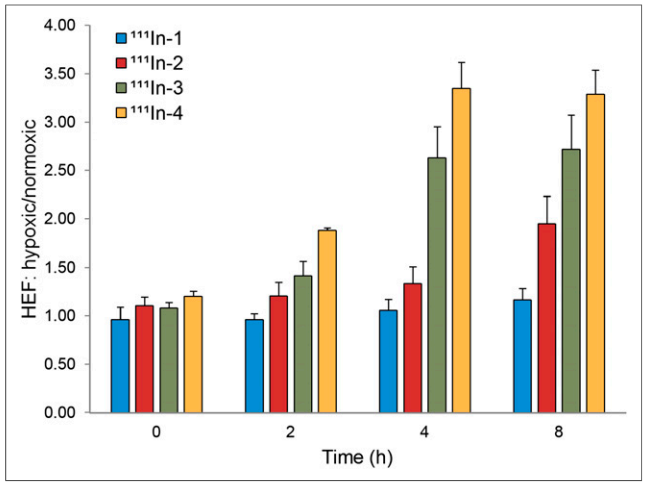

FIGURE 3. HEF ratios for efflux studies of ^{111}In-BB2r–targeted radioconjugates under normoxic (95% air, 5% CO_2) and hypoxic (94.9% N_2, 0.1% O_2, 5% CO_2) conditions. Values are mean ± SD (n = 5).

poor binding affinities, severely impeding internalization of these conjugates. In this study, an extended linker (8-AOC) was incorporated between the 2-nitroimidazole-amino-acid residue and the pharmacophore. The BB2r affinities of (1–4) natural indium–labeled and –unlabeled conjugates versus [^{125}I-Tyr$_4$] BBN were performed for the gastrin-releasing peptide receptor using the PC-3 cell line. All ^{nat}In-BBN conjugates demonstrated nanomolar binding affinity. On the basis of these results, the incorporation of the 8-AOC linker has eliminated the detrimental impact of a 2-NIAA side chain on pharmacophore binding.

Internalization and efflux studies demonstrated that the clearance rate of the radioconjugates containing 2-nitroimidazole was substantially lower relative to the control under hypoxic conditions. Specifically, at the 8-h time point for **^{111}In-1, ^{111}In-2, ^{111}In-3,** and **^{111}In-4,** 6.6%, 25.4%, 35.9%, and 39.7%, respectively, more retention was observed under hypoxic conditions than normoxic conditions. **^{111}In-3** and **^{111}In-4,** which have more than one 2-nitroimidazole (2 and 3, respectively), exhibited a higher retention effect than **^{111}In-2,** which has only one 2-nitroimidazole. Inclusion of more than one hypoxia-trapping moiety may increase the chances for the 2-nitroimidazole–containing radioconjugates

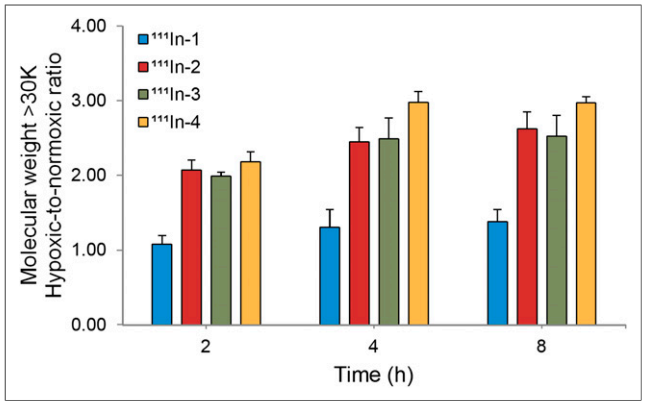

FIGURE 4. Protein-association studies under normoxic (95% air, 5% CO_2) and hypoxic (94.9% N_2, 0.1% O_2, 5% CO_2) conditions in PC-3 cells. Values are mean ± SD (n = 5).

TABLE 2
Biodistribution Studies in PC-3 Tumor–Bearing SCID Mice

Tissue (%ID/g)	1 h after injection	4 h after injection	24 h after injection	48 h after injection	72 h after injection
^{111}In-1					
Blood	0.11 ± 0.22	0.00 ± 0.00	0.00 ± 0.00	0.00 ± 0.00	0.00 ± 0.00
Heart	0.00 ± 0.00	0.00 ± 0.00	0.00 ± 0.00	0.00 ± 0.00	0.00 ± 0.00
Lung	0.21 ± 0.40	0.02 ± 0.03	0.00 ± 0.00	0.00 ± 0.00	0.00 ± 0.00
Liver	0.40 ± 0.32	0.09 ± 0.11	0.03 ± 0.03	0.00 ± 0.00	0.00 ± 0.00
Pancreas	70.96 ± 15.88	37.17 ± 10.52	12.07 ± 3.05	6.51 ± 2.26	0.00 ± 0.00
Stomach	5.87 ± 3.63	1.02 ± 0.72	0.34 ± 0.26	0.11 ± 0.23	0.00 ± 0.00
Small intestine (%ID)	8.15 ± 2.93	2.04 ± 0.59	0.96 ± 0.52	0.66 ± 0.18	0.02 ± 0.04
Large intestine (%ID)	5.07 ± 1.26	4.74 ± 2.08	1.62 ± 0.54	1.71 ± 0.87	0.46 ± 0.28
Kidney	13.41 ± 5.84	4.82 ± 1.60	2.18 ± 0.67	1.38 ± 1.01	0.76 ± 0.67
Tumor	5.82 ± 2.63	2.16 ± 1.01	1.32 ± 0.62	0.83 ± 0.48	0.09 ± 0.10
Muscle	0.00 ± 0.00	0.00 ± 0.00	0.00 ± 0.00	0.00 ± 0.00	0.00 ± 0.00
Bone	0.00 ± 0.00	0.00 ± 0.00	0.00 ± 0.00	0.00 ± 0.00	0.00 ± 0.00
Brain	0.00 ± 0.00	0.00 ± 0.00	0.00 ± 0.00	0.00 ± 0.00	0.00 ± 0.00
Excretion* (%ID)	35.88 ± 14.38	82.06 ± 4.65	91.07 ± 1.75	93.42 ± 3.26	98.44 ± 0.48
^{111}In-2					
Blood	1.21 ± 0.61	0.00 ± 0.00	0.02 ± 0.02	0.00 ± 0.00	0.00 ± 0.00
Heart	0.00 ± 0.00	0.00 ± 0.00	0.00 ± 0.00	0.00 ± 0.00	0.00 ± 0.00
Lung	1.21 ± 0.98	0.00 ± 0.00	0.00 ± 0.00	0.00 ± 0.00	0.00 ± 0.00
Liver	0.87 ± 0.38	0.15 ± 0.05	0.13 ± 0.05	0.08 ± 0.01	0.06 ± 0.02
Pancreas	33.70 ± 27.11	14.01 ± 13.97	1.98 ± 1.35	0.25 ± 0.17	0.22 ± 0.12
Stomach	1.51 ± 1.69	0.49 ± 0.20	0.06 ± 0.08	0.07 ± 0.09	0.04 ± 0.08
Small intestine (%ID)	4.62 ± 1.42	1.44 ± 0.61	0.23 ± 0.10	0.12 ± 0.06	0.02 ± 0.02
Large intestine (%ID)	2.02 ± 0.7	3.82 ± 1.11	0.57 ± 0.18	0.35 ± 0.14	0.15 ± 0.04
Kidney	14.88 ± 4.55	5.09 ± 1.70	3.74 ± 1.65	2.03 ± 0.42	2.66 ± 0.73
Tumor	6.06 ± 3.35	1.89 ± 0.92	1.08 ± 0.49	0.58 ± 0.24	0.41 ± 0.07
Muscle	1.69 ± 1.72	0.12 ± 0.25	0.00 ± 0.00	0.00 ± 0.00	0.00 ± 0.00
Bone	0.71 ± 0.42	0.14 ± 0.15	0.00 ± 0.00	0.00 ± 0.00	0.00 ± 0.00
Brain	0.02 ± 0.05	0.00 ± 0.00	0.00 ± 0.00	0.00 ± 0.00	0.00 ± 0.00
Excretion* (%ID)	17.26 ± 15.53	81.24 ± 8.28	94.89 ± 0.67	96.10 ± 0.61	95.90 ± 0.95
^{111}In-4					
Blood	0.75 ± 0.54	0.00 ± 0.00	0.00 ± 0.00	0.00 ± 0.00	0.00 ± 0.00
Heart	0.73 ± 1.46	0.00 ± 0.00	0.00 ± 0.00	0.00 ± 0.00	0.00 ± 0.00
Lung	0.61 ± 1.04	0.41 ± 0.82	0.00 ± 0.00	0.00 ± 0.00	0.00 ± 0.00
Liver	0.38 ± 0.36	0.30 ± 0.24	0.20 ± 0.45	0.45 ± 0.33	0.01 ± 0.02
Pancreas	33.04 ± 19.50	7.73 ± 2.70	0.62 ± 1.25	0.06 ± 0.12	0.00 ± 0.00
Stomach	0.50 ± 0.75	0.00 ± 0.00	0.00 ± 0.00	0.00 ± 0.00	0.00 ± 0.00
Small intestine (%ID)	3.18 ± 1.77	1.00 ± 0.59	0.25 ± 0.18	0.01 ± 0.01	0.09 ± 0.14
Large intestine (%ID)	2.16 ± 0.94	2.38 ± 1.05	0.83 ± 0.16	0.57 ± 0.33	0.24 ± 0.27
Kidney	17.90 ± 10.88	25.79 ± 4.66	23.40 ± 12.33	12.87 ± 2.76	8.83 ± 5.69
Tumor	2.80 ± 1.18	1.43 ± 0.62	0.92 ± 0.46	0.69 ± 0.53	0.60 ± 0.40
Muscle	0.00 ± 0.00	0.00 ± 0.00	0.00 ± 0.00	0.00 ± 0.00	0.00 ± 0.00
Bone	0.00 ± 0.00	0.00 ± 0.00	0.00 ± 0.00	0.00 ± 0.00	0.00 ± 0.00
Brain	0.00 ± 0.00	0.00 ± 0.00	0.00 ± 0.00	0.00 ± 0.00	0.00 ± 0.00
Excretion* (%ID)	61.95 ± 23.27	80.86 ± 2.63	87.21 ± 2.75	91.55 ± 1.73	93.85 ± 2.78

*Excretion values were calculated using activity values associated with excreted urine, bladder, and fecal material contents at time of sacrifice.

Organ uptake values expressed as %ID/g and values are mean ± SD (n = 4) unless otherwise noted.

to form protein adducts, thus enhancing the long-term retention of the radioconjugate in the cell. Ultimately, further investigation into the identification and quantification of the protein adduct is needed to obtain a clearer understanding of the mechanism involved in this process. Also, **^{111}In-1** exhibited a slightly lower clearance rate under hypoxic conditions, which could be due to the decreased metabolic rate under hypoxic conditions (*9*). With respect to the HEF, significantly higher retention in hypoxic than normoxic cells was observed for **^{111}In-2–4** at the 2-h time point. The HEF continued to increase for **^{111}In-1** and **^{111}In-2** throughout the experiments but remained constant for **^{111}In-3** and **^{111}In-4** after the 4-h time point. A strong positive linear relationship between the HEF and the number of 2-nitroimidazoles incorporated was confirmed for the 8-h time points.

Cellular protein analysis of the control radioconjugate **^{111}In-1** demonstrated minimal hypoxic-to-normoxic cellular protein-association ratios, which are likely due to reversible, nonspecific binding. For the 2-nitroimidazole–containing BB2r-targeted conjugates, up to a 2-fold increase was observed under hypoxic conditions. These results suggest that the significantly higher

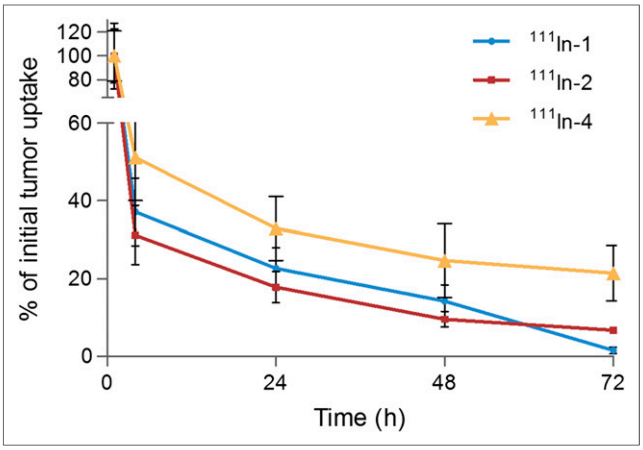

FIGURE 5. Percentage tumor retention of **^{111}In-1, ^{111}In-2,** and **^{111}In-4** in PC-3 tumor–bearing SCID mice. Values are mean ± SEM (n = 4).

protein-association ratio of 2-nitroimidazole–containing radioconjugates is due, at least in part, to the irreversible binding to intracellular proteins, which is consistent with the known trapping mechanism of 2-nitroimidazole.

The in vivo biodistribution of each radioconjugate was investigated in PC-3 tumor–bearing SCID mice, except for **^{111}In-3** because this radioconjugate had efflux and protein-association properties similar to **^{111}In-4.** At 1 h after injection, **^{111}In-1** and **^{111}In-2** share comparable tumor uptake, 5.82 ± 2.63 and 6.06 ± 3.35 %ID/g, respectively. However, a substantially lower tumor uptake (2.80 ± 1.18 %ID/g) was observed for **^{111}In-4,** which has three 2-nitroimidazoles incorporated. Given the similar uptake of **^{111}In-2** and **^{111}In-4** in the BB2r-positive pancreas, the reason behind the reduced tumor uptake is unclear. At 4 h after injection, most of the radioconjugates were cleared through the renal or urinary system (80–82 %ID), which is consistent with other investigations of BB2r-targeted radioconjugates (*19*). By the 72-h postinjection time point, the radioconjugates were largely cleared from most tissues, including the pancreas (*20*). Significant tumor retention enhancement was observed at 72 h after injection for radioconjugates **^{111}In-2** and **^{111}In-4.** Specifically, 6.7% and 21.0% of the initial 1-h uptake in tumor was retained for **^{111}In-2** and **^{111}In-4,** compared with only 1.5% remaining for the control **^{111}In-1.** However, the hypoxia burden of each tumor is unknown, limiting the ability to fully interpret the relationship between tumor retention effect and incorporation of the hypoxia-trapping moiety. The hypoxia burden in tumor xenograft mouse models has been shown to increase (modest correlation) with an increase in tumor size, but this trend is highly dependent on the cell line (*21*). Linear regression analysis of the %ID/g retention of our radioconjugates in PC-3 tumors versus tumor weight revealed no correlation between retention and tumor size. Interestingly, in the clinic, the extent of hypoxia is independent of tumor size in a variety of human cancers, including head and neck, cervical, and lung (*22–24*). Further study to correlate the tumor hypoxia burden with radioconjugate retention is ongoing. Significantly lower tumor and pancreas uptake caused by the coinjection of an excess of unlabeled conjugate **4** indicates that accumulation of **^{111}In-4** is largely mediated by the BB2r.

It is interesting to note the unusually high kidney retention for 2-nitroimidazole–containing conjugates relative to the control conjugate. This is particularly true of **^{111}In-4,** with a kidney retention of 8.83 ± 5.69 %ID/g at 72 h after injection. This renal retention value is higher, to the best of our knowledge, than any reported research related to bombesin or 2-nitroimidazole–based radioconjugates (*5,19,25,26*). Renal retention of radiolabeled targeting peptide has long been addressed as one of the dose-limiting factors in radionuclide therapy, and various mechanisms have been demonstrated to be involved in high renal uptake (*27*). Cationic peptides are preferentially reabsorbed by the proximal tubules because of the anionic binding sites on the brush border membrane (*28,29*). Megalin and cubilin are known to be associated with the proximal tubular reabsorption of structurally different proteins, peptides, and drugs (*30*). Moreover, low or very low tissue oxygen tensions exist under physiologic conditions in the kidneys, facilitating urine concentration (*31*). Coinfusion of competitive inhibitors such as lysine, arginine, and succinylated gelatin can reduce the reabsorption by endocytosis or transporters (*32–34*). In preliminary coinjection blocking studies (data not shown), both EF5 (a 2-nitroimidazole–based hypoxia marker) and lysine coinjection with **^{111}In-4** can reduce the retention of radioconjugates in the kidneys. Further studies are needed to fully understand the mechanism of kidney retention of hypoxia-trapping enhanced bombesin conjugates to develop specific methods to reduce the renal toxicity.

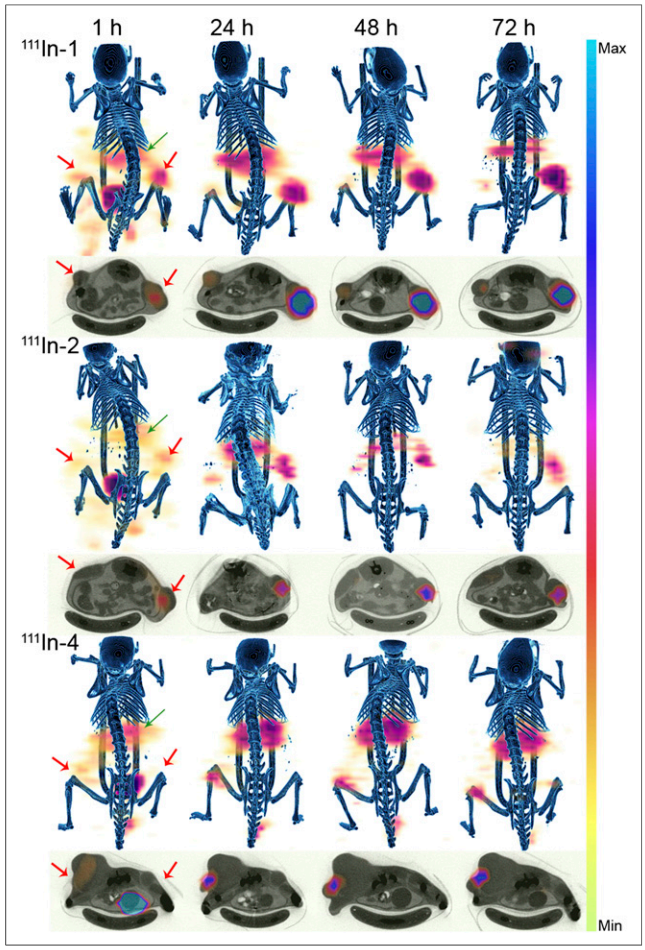

FIGURE 6. Fused micro-SPECT/CT and axial images of **^{111}In-1, ^{111}In-2,** and **^{111}In-4** in PC-3 tumor–bearing mice at 1, 24, 48, and 72 h after injection. Tumors and kidneys are indicated by red and green arrows, respectively. Max = maximum; Min = minimum.

Micro-SPECT/CT images of all radioconjugates using PC-3 tumor–bearing mice at 1 h after injection (Fig. 6), showing significant abdominal uptake, are consistent with the data obtained from biodistribution studies. The PC-3 tumor xenografts in all mice are easily visualized. For the **^{111}In-4** radioconjugates, containing three 2-nitroimidazoles, significant activity in the kidneys was observed, strongly agreeing with previously established biodistribution data.

CONCLUSION

We have synthesized 3 BB2r-targeted radioconjugates with 2-nitroimidazole hypoxia-trapping moieties incorporated to enhance the retention in hypoxic cancer cells. In vitro competitive binding studies indicate that inclusion of extended linker 8-AOC eliminated the detrimental effect on binding affinity that was determined in our previous report. The 2-nitroimidazole–trapping moieties containing BB2r-targeted agents demonstrated significantly higher retention and protein-association properties in hypoxic than in normoxic PC-3 cells. In vivo biodistribution studies revealed great potential of incorporated trapping moieties to increase the residence time of BB2r-targeted agents in a PC-3 xenograft tumor. Further works are needed to clarify the mechanisms of increased retention effects at the molecular level and to correlate the tumor hypoxia burden with the retention efficacy.

DISCLOSURE

The costs of publication of this article were defrayed in part by the payment of page charges. Therefore, and solely to indicate this fact, this article is hereby marked “advertisement” in accordance with 18 USC section 1734. This study was supported by the National Cancer Institute (5 R00 CA137147) and the National Center for Research Resources (8 P20 GM103480). No other potential conflict of interest relevant to this article was reported.

ACKNOWLEDGMENT

We thank Dr. Katherine Estes for assistance in SPECT/CT imaging and the Bioimaging Core at UNMC.

REFERENCES

1. Siegel R, Naishadham D, Jemal A. Cancer statistics, 2012. *CA Cancer J Clin.* 2012;62:10–29.
2. Gugger M, Reubi JC. Gastrin-releasing peptide receptors in non-neoplastic and neoplastic human breast. *Am J Pathol.* 1999;155:2067–2076.
3. Markwalder R, Reubi JC. Gastrin-releasing peptide receptors in the human prostate: relation to neoplastic transformation. *Cancer Res.* 1999;59:1152–1159.
4. Abd-Elgaliel WR, Gallazzi F, Garrison JC, et al. Design, synthesis, and biological evaluation of an antagonist: bombesin analogue as targeting vector. *Bioconjug Chem.* 2008;19:2040–2048.
5. Garrison JC, Rold TL, Sieckman GL, et al. In vivo evaluation and small-animal PET/CT of a prostate cancer mouse model using ^{64}Cu bombesin analogs: side-by-side comparison of the CB-TE2A and DOTA chelation systems. *J Nucl Med.* 2007;48:1327–1337.
6. Zhang X, Cai W, Cao F, et al. ^{18}F-labeled bombesin analogs for targeting GRP receptor-expressing prostate cancer. *J Nucl Med.* 2006;47:492–501.
7. Hoffman TJ, Gali H, Smith CJ, et al. Novel series of ^{111}In-labeled bombesin analogs as potential radiopharmaceuticals for specific targeting of gastrin-releasing peptide receptors expressed on human prostate cancer cells. *J Nucl Med.* 2003;44:823–831.
8. Milosevic M, Warde P, Ménard C, et al. Tumor hypoxia predicts biochemical failure following radiotherapy for clinically localized prostate cancer. *Clin Cancer Res.* 2012;18:2108–2114.
9. Höckel M, Vaupel P. Tumor hypoxia: definitions and current clinical, biologic, and molecular aspects. *J Natl Cancer Inst.* 2001;93:266–276.
10. Nunn A, Linder K, Strauss HW. Nitroimidazoles and imaging hypoxia. *Eur J Nucl Med.* 1995;22:265–280.
11. Krohn KA, Link JM, Mason RP. Molecular imaging of hypoxia. *J Nucl Med.* 2008;49(suppl):129S–148S.
12. Bolton JL, McClelland RA. Kinetics and mechanism of the decomposition in aqueous solutions of 2-(hydroxyamino) imidazoles. *J Am Chem Soc.* 1989;111:8172–8181.
13. Grosu AL, Souvatzoglou M, Roper B, et al. Hypoxia imaging with FAZA-PET and theoretical considerations with regard to dose painting for individualization of radiotherapy in patients with head and neck cancer. *Int J Radiat Oncol Biol Phys.* 2007;69:541–551.
14. Mannan RH, Somayaji VV, Lee J, Mercer JR, Chapman JD, Wiebe LI. Radioiodinated 1-(5-iodo-5-deoxy-beta-D-arabinofuranosyl)-2-nitroimidazole (iodoazomycin arabinoside: IAZA): a novel marker of tissue hypoxia. *J Nucl Med.* 1991;32:1764–1770.
15. Koh WJ, Rasey JS, Evans ML, et al. Imaging of hypoxia in human tumors with [F-18]fluoromisonidazole. *Int J Radiat Oncol Biol Phys.* 1992;22:199–212.
16. Wagh NK, Zhou Z, Ogbomo SM, Shi W, Brusnahan SK, Garrison JC. Development of hypoxia enhanced ^{111}In-labeled bombesin conjugates: design, synthesis, and in vitro evaluation in PC-3 human prostate cancer. *Bioconjug Chem.* 2012;23:527–537.
17. Brown JM, Wilson WR. Exploiting tumour hypoxia in cancer treatment. *Nat Rev Cancer.* 2004;4:437–447.
18. Raleigh JA, Koch CJ. Importance of thiols in the reductive binding of 2-nitroimidazoles to macromolecules. *Biochem Pharmacol.* 1990;40:2457–2464.
19. Garrison JC, Rold TL, Sieckman GL, et al. Evaluation of the pharmacokinetic effects of various linking group using the ^{111}In-DOTA-X-BBN (7-14) NH2 structural paradigm in a prostate cancer model. *Bioconjug Chem.* 2008;19:1803–1812.
20. Waser B, Eltschinger V, Linder K, Nunn A, Reubi JC. Selective in vitro targeting of GRP and NMB receptors in human tumours with the new bombesin tracer 177 Lu-AMBA. *Eur J Nucl Med Mol Imaging.* 2007;34:95–100.
21. Wang J, Klem J, Wyrick JB, et al. Detection of hypoxia in human brain tumor xenografts using a modified comet assay. *Neoplasia.* 2003;5:288–296.
22. Nordsmark M, Bentzen SM, Overgaard J. Measurement of human tumour oxygenation status by a polarographic needle electrode: an analysis of inter-and intratumour heterogeneity. *Acta Oncol.* 1994;33:383–389.
23. Rasey JS, Koh W-J, Grierson JR, Grunbaum Z, Krohn KA. Radiolabeled fluoromisonidazole as an imaging agent for tumor hypoxia. *Int J Radiat Oncol Biol Phys.* 1989;17:985–991.
24. Fyles A, Milosevic M, Hedley D, et al. Tumor hypoxia has independent predictor impact only in patients with node-negative cervix cancer. *J Clin Oncol.* 2002;20:680–687.
25. Melo T, Duncan J, Ballinger JR, Rauth AM. BRU59-21, a second-generation ^{99m}Tc-labeled 2-nitroimidazole for imaging hypoxia in tumors. *J Nucl Med.* 2000;41:169–176.
26. Evans SM, Kachur AV, Shiue CY, et al. Noninvasive detection of tumor hypoxia using the 2-nitroimidazole [^{18}F] EF1. *J Nucl Med.* 2000;41:327–336.
27. Vegt E, de Jong M, Wetzels JF, et al. Renal toxicity of radiolabeled peptides and antibody fragments: mechanisms, impact on radionuclide therapy, and strategies for prevention. *J Nucl Med.* 2010;51:1049–1058.
28. Behr TM, Sharkey RM, Juweid ME, et al. Reduction of the renal uptake of radiolabeled monoclonal antibody fragments by cationic amino acids and their derivatives. *Cancer Res.* 1995;55:3825–3834.
29. Pimm MV, Gribben SJ. Prevention of renal tubule re-absorption of radiometal (indium-111) labelled Fab fragment of a monoclonal antibody in mice by systemic administration of lysine. *Eur J Nucl Med.* 1994;21:663–665.
30. Christensen EI, Birn H. Megalin and cubilin: multifunctional endocytic receptors. *Nat Rev Mol Cell Biol.* 2002;3:256–266.
31. Brezis M, Rosen S. Hypoxia of the renal medulla: its implications for disease. *N Engl J Med.* 1995;332:647–655.
32. de Jong M, Rolleman EJ, Bernard BF, et al. Inhibition of renal uptake of indium-111-DTPA-octreotide in vivo. *J Nucl Med.* 1996;37:1388–1392.
33. Rolleman EJ, Valkema R, de Jong M, Kooij PP, Krenning EP. Safe and effective inhibition of renal uptake of radiolabelled octreotide by a combination of lysine and arginine. *Eur J Nucl Med Mol Imaging.* 2003;30:9–15.
34. van Eerd JE, Vegt E, Wetzels JF, et al. Gelatin-based plasma expander effectively reduces renal uptake of ^{111}In-octreotide in mice and rats. *J Nucl Med.* 2006;47:528–533.

JNM The Journal of NUCLEAR MEDICINE

Synthesis and In Vitro and In Vivo Evaluation of Hypoxia-Enhanced ^{111}In-Bombesin Conjugates for Prostate Cancer Imaging

Zhengyuan Zhou, Nilesh K. Wagh, Sunny M. Ogbomo, Wen Shi, Yinnong Jia, Susan K. Brusnahan and Jered C. Garrison

J Nucl Med. 2013;54:1605-1612.
Published online: July 29, 2013.
Doi: 10.2967/jnumed.112.117986

The Journal of Nuclear Medicine is published monthly.
SNMMI | Society of Nuclear Medicine and Molecular Imaging
1850 Samuel Morse Drive, Reston, VA 20190.
(Print ISSN: 0161-5505, Online ISSN: 2159-662X)

SNMMI SOCIETY OF NUCLEAR MEDICINE AND MOLECULAR IMAGING